

Comparing the Therapeutic Mechanism and Immune Response of Human and Mouse Mesenchymal Stem Cells in Immunocompetent Mice With Acute Liver Failure

Chang-Hung Wang¹, Che-Yi Chen¹, Kai-Hung Wang², An-Pei Kao³, Yi-Jou Chen⁴, Pei-Hsuan Lin⁴, Michael Chen⁴, Tung-Yun Wu¹, Jing-Jy Cheng^{1,5}, Kuan-Der Lee^{6,7,*}, Kuo-Hsiang Chuang^{1,4,8,9,*} 

¹Ph.D. Program in Clinical Drug Development of Herbal Medicine, College of Pharmacy, Taipei Medical University, Taipei City, Taiwan

²Department of Obstetrics and Gynecology, Kuo General Hospital, Tainan City, Taiwan

³Research and Development, Stemforce Biotechnology Company Limited, Chiayi City, Taiwan

⁴Graduate Institute of Pharmacognosy, College of Pharmacy, Taipei Medical University, Taipei City, Taiwan

⁵Division of Basic Chinese Medicine, National Research Institute of Chinese Medicine, Taipei City, Taiwan

⁶Department of Medical Research and Cell Therapy and Regenerative Medicine Center, Taichung Veterans General Hospital, Taichung City, Taiwan

⁷Office of Research and Development, TMU Research Center of Cell Therapy and Regeneration Medicine, Taipei Medical University, Taipei City, Taiwan

⁸Department of Traditional Chinese Medicine, Traditional Herbal Medicine Research Center, Taipei Medical University Hospital, Taipei City, Taiwan

⁹Drug Development and Value Creation Research Center, Kaohsiung Medical University, Kaohsiung City, Taiwan

*Corresponding author: Kuan-Der Lee, M.D. Ph.D., 1650 Taiwan Boulevard Sect. 4, Taichung 407, Taiwan. Tel: +886 4 2359 2525; Email: kdlee1964@gmail.com; or, Kuo-Hsiang Chuang, Ph.D., 250 Wu-Hsing Street, Taipei City 110, Taiwan. Tel: +886 2 2736 1661; Email: khchuang@tmu.edu.tw

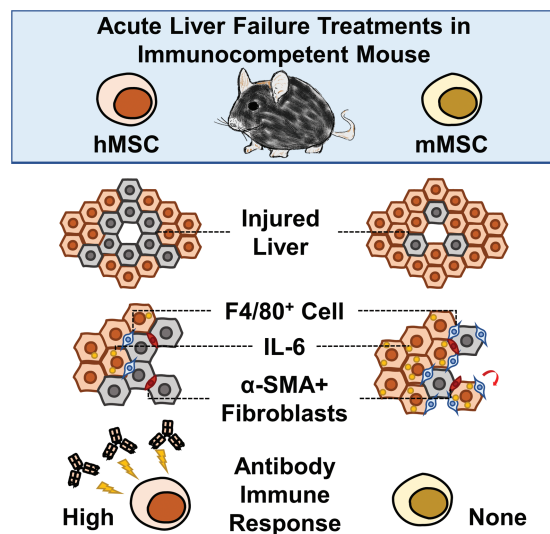
Abstract

Current mesenchymal stem cell (MSC) research is based on xenotransplantation of human MSCs (hMSCs) in immunodeficient mice and cannot comprehensively predict MSC repair mechanisms and immunomodulatory effects in damaged tissue. This study compared the therapeutic efficacy, mechanisms, and immune response of hMSCs and mouse MSCs (mMSCs) in immunocompetent mice with CCl₄-induced acute liver failure. mMSCs maintained F4/80⁺ hepatic macrophage recruitment into the damaged liver region, increased IL-6-dependent hepatocyte proliferation, and reduced inflammatory TNF- α cytokine secretion. Moreover, mMSCs reduced α -SMA⁺ myofibroblast activation by lowering TGF- β 1 accumulation in damaged liver tissue. In contrast, hMSCs lowered TNF- α and TGF- β 1 by reducing the recruitment of F4/80⁺ hepatic macrophages, which lost the ability to remove debris and induce IL-6 liver regeneration. Finally, hMSCs, but not mMSCs, caused a significant antibody response in immunocompetent mice; therefore, hMSCs are unsuitable for long-term MSC studies. This comparative study provides reference information for further MSC studies of immunocompetent mice.

Key words: mesenchymal stem cells; immunomodulatory; IL-6, F4/80; liver regeneration; liver fibrosis.

Graphical Abstract

The mMSCs treatment showed less injured liver area than the hMSCs. Liver regeneration relies on F4/80⁺ macrophage and IL-6-dependent hepatocyte proliferation. The mMSC, but not hMSC, maintained the F4/80⁺ macrophage recruitment and IL-6-dependent hepatocyte proliferation. Both the hMSC and mMSC reduced α -SMA⁺ fibroblast activation. However, the hMSC showed a high antibody immune response in immunocompetent mice with acute liver failure.



Received: 4 July 2022; Accepted: 30 November 2022.

© The Author(s) 2023. Published by Oxford University Press.

This is an Open Access article distributed under the terms of the Creative Commons Attribution-NonCommercial License (<https://creativecommons.org/licenses/by-nc/4.0/>), which permits non-commercial re-use, distribution, and reproduction in any medium, provided the original work is properly cited. For commercial re-use, please contact journals.permissions@oup.com.

Significance Statement

The immunodeficiency mice are generally used to evaluate the hMSC therapeutic efficacy but are absent from investigating MSC immune-modulatory effects. Our study compared the adipose-tissue-derived hMSC and mMSC with therapeutic efficacy and liver regenerative mechanisms in immunocompetent mice with acute liver failure. The measurement focused on the liver F4/80⁺ hepatic macrophage recruitment, IL-6-dependent hepatocyte regeneration, TNF- α inflammation, pro-fibrotic molecule activation, and anti-MSC immune response. The results provide the differences between hMSC and mMSC treatments and help us understand and design further MSC therapy in immunocompetent mice with acute liver failure.

Introduction

Acute liver failure is a lethal symptom with severe cell apoptosis and necrosis in the patient's liver, but an effective treatment for it is still lacking. Current treatments focus on removing liver toxicity factors and lowering the liver metabolite burden to allow liver self-regeneration. However, the supporting therapies are not sufficient to treat severe acute liver failure. The immune microenvironment has been discussed as benefiting liver regeneration.^{1,2} In the early stage of acute liver failure, innate immune cells, especially hepatic macrophages—Kupffer cells—rapidly recruit to the necrotic area of the liver as scavengers of phagocytotic cell debris.³ When hepatic macrophages are recruited to the damaged areas of the liver, they secrete pro-inflammatory cytokines, which induce blood monocytes to differentiate into pro-inflammatory macrophages.^{2,4} Persistent inflammation delays anti-inflammatory macrophage differentiation and halts liver regeneration. Mesenchymal stem cells (MSCs) have been investigated as an effective regenerative source to replace injured, inflamed, or malfunctioning tissue by recovering liver tissue homeostasis.⁵ In addition, pro-inflammatory cytokine-induced MSCs promote anti-inflammatory macrophages.⁶ Therefore, the immunomodulatory therapeutic potential of MSCs should be considered in the early stage of acute liver failure.

MSC therapies have been widely studied for their beneficial effect on liver diseases.^{7,8} Therapeutic efficiency assessments of MSCs involve cell differentiation potency and the MSC secretome, including soluble cytokines, growth factors, hormones, and the miRNA exosome that influence damaged cells, immune cells, and cells participating in tissue recovery.⁹ However, a comprehensive therapeutic model of human MSC (hMSC) therapies is difficult to provide for immunocompetent mice because the possible immune rejection may defect MSC regeneration, which has been reported in pig and rat xenotransplantation models.¹⁰ Immunodeficient mouse models are chosen for evaluating the therapeutic effects of hMSCs. Due to the lack of an immune system, immunodeficient mouse models provide insufficient information to predict immunomodulatory effects in humans. Therefore, it should use allogeneic mouse MSC (mMSC), which provides sufficient information to explore therapeutic effects and mechanisms in immunocompetent acute liver failure mouse models.

This study compared the therapeutic efficacy, immunomodulatory effects, and immune responses of hMSC and mMSCs in immunocompetent mice with acute liver failure. Hepatocyte differentiation potency and liver injury conditions were investigated to evaluate the efficacy of hMSC and mMSC therapies. In addition, the hMSC and mMSC treatments were analyzed for liver regeneration-related and liver fibrosis factors to explore immunomodulatory effects.

Finally, multiple dosage injections of hMSCs and mMSCs were administered to compare the immunogenicity and immunological memory effects of MSC therapies in a long-term study.

Materials and Methods

Materials

The materials are detailed in supplementary information ([Supplementary Table S1](#)).

Animals

C57BL/6JNarl mice were acquired from the National Laboratory Animal Center, Taiwan. Seven-week-old female C57BL/6JNarl mice were bred and housed at Taipei Medical University. All animal procedures were approved by the Taipei Medical University Institutional Animal Care and Use Committee.

Isolation and Culture of Mouse Adipose Tissue-Derived Mesenchymal Stem Cells

Twelve-week-old male C57BL/6JNarl mice were humanely sacrificed, and their gonadal adipose tissue was digested with dispase II (4 units/g) and collagenase type II (1000 CDU/g) at 37°C for 1 h. After digestion, we collected the stromal vascular fraction (SVF) by 400 \times g centrifugation. The SVF was cultured starting at low cell density (200 cells/cm²) and cell confluence under 80% in α MEM with 10% fetal bovine serum (FBS), 1% antibiotic-antimycotic solution, 0.1% gentamicin sulfate, 2 mM N-acetyl-L-cysteine, and 0.2 mM L-ascorbic acid 2-phosphate at 37°C, 5% CO₂, and 100% relative humidity (RH). The mMSCs were cultured for \leq 3 passages for further study.

Culture of Human Adipose Tissue-Derived Mesenchymal Stem Cells

Female human adipose tissue-derived MSCs were purchased from LONZA. The MSCs were cultured starting at low cell density (200 cells/cm²) and cell confluence under 80% in hMSC SF1 basal medium at 37°C, 5% CO₂, 1% antibiotic-antimycotic solution, 0.1% gentamicin sulfate, 2 mM N-acetyl-L-cysteine, 0.2 mM L-ascorbic acid 2-phosphate, and 100% RH. The hMSCs were cultured for \leq 3 passages for further study.

Evaluation of MSC Self-Renewal and Cell Doubling Time

The self-renewal ability of human and mouse MSCs was determined using the colony-forming unit-fibroblast (CFU-F) assay. The hMSCs and mMSCs were seeded at 200 cells/dish (55 cm² growth area). After 10 days, the cells were stained with 0.9% crystal violet for 10 minutes at room temperature

and then washed with tap water for 10 minutes. The cells were analyzed for the number of colonies.

Cell doubling time was evaluated using the cumulative population doubling level (CPDL) method.¹¹ The human and mouse MSCs were seeded at 1×10^4 cells/dish (55 cm² growth area). When cell confluence was approximately 80%, the cells were counted as total cell numbers. The CPDL was calculated using the following formula:

$$CPDL = 3.32 (\log UCY - \log I) + X,$$

where UCY was cell yield, *I* was the number of cells used to initiate the subculture, and *X* was the doubling level used in the previous subculture.

Flow Cytometry

Human MSC markers were detected using CD90, CD105, CD73, CD34, CD45, CD11b, CD19, and HLA-DR antibodies. Mouse MSC markers were detected using CD105, CD29, CD44, SCA-1, CD31, CD45, and TER-119 antibodies. In the extracellular staining groups, dead cells from human or mouse MSCs were excluded by 10 µg/mL propidium iodide staining. Intracellular staining of human CD73 and mouse MSC CD29 was performed by fixing with 4% paraformaldehyde and permeabilizing the cells with 0.1% Triton X-100 for 10 minutes at room temperature. All unconjugated antibodies were detected by fluorescein-conjugated antibodies. Antibody incubation time was 1 h on ice. The human and mouse MSCs were analyzed using a spectral analyzer (SONY SA3800). The data were analyzed using FlowJo software.

MSC Differentiation

The MSC trilineage differentiations are detailed in [Supplementary Material](#).

Hepatocyte differentiation was performed in 2 steps in medium.¹² First (day 0), the hMSCs and mMSCs were plated at 1×10^5 cells/well in growth medium and 6-well cell culture plates. When MSCs were propagated to 90% cell confluence, the mouse MSCs were treated with α MEM with 10% FBS and 20 µM 5-azacytidine for 24 h, and then kept in refreshed medium with DMEM low glucose/MEM ratio (1/1), 2% FBS, 1% antibiotic-antimycotic solution, 0.1% gentamicin sulfate, 0.1% BSA, 5.55 mM D-galactose, 0.3 mM L-ornithine HCl, 4.99 mM HEPES, 1.25 mM nicotinamide, 0.2 µM ZnCl₂, 0.04 µM CuSO₄ × 5H₂O, 0.13 µM ZnSO₄ × 7H₂O, 0.074 µM MnSO₄ × H₂O, 50 nM dexamethasone, 1% insulin-transferrin-selenium supplement, 20 ng/mL EGF, and 40 ng/mL HGF for 2 weeks. Cell morphology demonstrated a binucleated type. After 2 weeks of differentiation, the cells were lysed by RIPA buffer for cytochrome P450 3A4 (CYP3A4) and phosphoenolpyruvate carboxykinase 1 (PCK1) expression analysis.

Acute Liver Failure Induction in Mice and MSC Transplantation

Eight-week-old female C57BL/6JNarl mice were intraperitoneally injected with CCl₄ solution, which was mixed with olive oil for a final concentration of 10% (v/v) CCl₄. The CCl₄ dosages were determined by mouse body weight (15 µL CCl₄/20 g mouse). After 24 h of induction of acute liver failure, human and mouse MSCs were intravenously injected into the tail vein of each mouse at 2×10^5 cells/mouse. After 72 h of induction of acute liver failure, the

mice were humanely sacrificed and their serum and organs were collected and body/organ weight was measured for further analysis. Alanine transaminase (ALT) and aspartate transaminase (AST) concentrations were evaluated using a VetTest Chemistry Analyzer.

Histology and Immunohistochemistry

Mouse livers were fixed in 10% NBF for 24 h. The fixed tissue was processed with an ethanol concentration gradient and xylene, then embedded in paraffin wax by an automated tissue processor (Shandon Excelsior, Thermo Fisher Scientific, UK). The paraffin-embedded liver tissue was sectioned at 3-7 µm thickness and stained with H&E. The results of H&E staining were obtained with a scanner (MIRAX SCAN). The injured regions of the liver were quantified by ImageJ.

Immunohistochemistry (IHC) sections were dewaxed with xylene and rehydrated with an ethanol concentration gradient and deionized water. The tissue sections were boiled in Tris-EDTA (TE) or 10 mM sodium citrate buffer for 10 minutes and cooled for 20-30 minutes. Endogenous peroxidase was deactivated using 0.3% H₂O₂ solution for 5 minutes at room temperature. The tissue sections were blocked in 10% goat serum and 1% BSA in PBST for 1 h at room temperature. Next, the liver tissue samples were stained with TNF- α , IL-6, F4/80, TGF- β 1, and α -SMA antibodies and HRP-conjugated antibodies for detection of the targets. DAB substrate and hematoxylin were used for marker detection and counterstaining. A micromount solution was used for section mounting. The sections subjected to IHC staining were observed under a microscope (TissueGnostics Axio Observer Z1). Liver sections were quantified with signal expression using HistoQuest software.

Evaluation of Human and Mouse MSC Immune Response

Eight-week-old female C57BL/6JNarl mice were intraperitoneally injected with a vector, human MSCs (2×10^6 cells) or mouse MSCs (2×10^6 cells) at weeks 0, 1, 2, and 20 (booster shot). The body weight of mice was measured and their plasma collected at weeks -1, 1, 2, 3, 19, and 21 for further immune response analysis.

Western Blotting

The differentiated human and mouse MSC hepatocyte samples were quantified for protein concentration using the BCA method. The proteins in the samples were electrophoretically separated with 10% SDS-PAGE (reducing condition), transferred to nitrocellulose blotting membranes, and blocked with 5% skim milk for 2 h at room temperature. For differentiation efficiency, CYP3A4, PCK1, and β -actin protein expression were analyzed using anti-human/mouse CYP3A4, PCK1, and β -actin antibodies and HRP conjugated antibodies with a chemiluminescent substrate. β -actin staining was performed after the application of a mild stripping solution (0.2 M glycine, 2.9 mM SDS, and 1% Tween20 at a pH of 2.2). Chemiluminescence results were acquired by SynGene GeneGnome 5. The CYP3A4, PCK1, and β -actin results were quantified by ImageJ.

ELISA Assays

The serum of mice with CCl₄-induced acute liver failure was evaluated with mouse IL- β , TNF- α , and IL-6 ELISA kits. The results were read using an EPOCH reader at an optical

density (OD) of 450 nm. The human and mouse MSC immune responses were determined using NIH3T3-, human MSC-, and mouse MSC-based ELISAs. NIH3T3, hMSCs, and mMSCs were seeded at 3×10^4 cells/well in 96-well CellBIND microplates, which reached 100% cell confluence after 24 h. Mice plasma samples were incubated with the cells for 1 h at room temperature for immune response. The HRP-conjugated anti-mouse IgG antibody and ABTS substrate were used for target detection. The absorbance was read with an EPOCH reader at an OD of 405 nm.

MSC Cell Viability Assay

The hMSCs, and mMSCs were seeded at 2000 cells/well in 96-well CellBIND microplates, which reached 20%-30% cell confluence after 24 h. The week 3 mice plasma samples were 50-fold diluted and treated with the cells for 48 h at 37°C, 5% CO₂, and 100% humidity. The cell viabilities were evaluated by cell ATP concentration by ATP luminescence Kit. The control mice plasma has 100% cell viability.

Quantification and Statistical Analysis

All data are shown as mean \pm SD. The CYP3A4 and PCK1 western blot results were analyzed using their β -actin cell loading control and normalized using the non-differentiation group, and differences were quantified by 2-tailed unpaired *t*-tests. Body weight under acute liver failure and immune response results of cell-based ELISA were analyzed with repeated measures of one-way ANOVA. The organ weights of mice were normalized using their body weights and represented as percentages. One-way ANOVA was used to analyze other data. Tukey's test corrected for multiple comparisons was used for hypothesis testing.

Results

Characterization of Human and Mouse Adipose-Derived Mesenchymal Stem Cells

The morphology, MSC markers, self-renewal ability, and cell population doubling level (CPDL) of hMSCs and mMSCs were analyzed. Both types of MSC demonstrated a spindle-shaped morphology (Fig. 1A). The hMSCs showed approximately 99% MSC purity—CD90 (100%), CD105 (99.6%), CD73 (99.1%), CD34 (0.1%), CD45 (0%), CD11b (0%), CD19 (0%), and HLA-DR (0.1%) (Fig. 1B)—and met the International Society for Cellular Therapy (ISCT) standards for hMSC markers.¹³ The mMSCs showed approximately 90% purity—CD105 (98.3%), CD29 (99.9%), CD44 (96.8%), SCA-1 (90.6%), CD31 (1.9%), CD45 (0.7%), and TER-119 (0.8%) (Fig. 1C)—and met the criteria for mMSC markers.¹⁴

To evaluate the self-renewal ability of hMSCs and mMSCs, we performed the colony-forming unit-fibroblast (CFU-F) assay. The results showed that the self-renewal ability of hMSCs was 38% (Supplementary Fig. S1A), whereas it was 83% for mMSCs (Supplementary Fig. S1B). The cell doubling time of hMSCs and mMSCs was evaluated using the CPDL. The hMSC doubling time was approximately once per day (Fig. 1D), whereas the mMSC doubling time was once per 2 days (Fig. 1E). The reason for the difference between hMSC and mMSC self-renewal was the difference in CPDL. The cell doubling time of hMSCs was shorter than that of mMSCs. Moreover, the CPDL results also showed that the hMSCs had limited self-renewal capacity.

Trilineage and Hepatocyte Differentiation Potency of Human and Mouse Mesenchymal Stem Cells

In this study, we focused on comparing the therapeutic mechanisms of adipose-derived human and mouse MSCs in mice with acute liver failure. We first needed to prove that both human and mouse MSCs had similar differentiation potency. According to the ISCT, MSCs have the potential to differentiate into trilineage cells, including adipocytes, osteoblasts, and chondrocytes. Therefore, both hMSCs and mMSCs can also differentiate into adipocytes, osteoblasts, and chondrocytes. Moreover, MSCs have been reported to show hepatocyte differentiation potency.^{15,16} We evaluated the *in vitro* hepatocyte differentiation potential of hMSCs and mMSCs as the source of hepatic repair cells.¹²

The results showed that hMSCs (Fig. 2A) and mMSCs (Fig. 2B) had trilineage differentiation potential. In the case of hepatocyte differentiation, both hMSCs and mMSCs showed polyploidization morphology; in Fig. 2C, the arrows indicate binucleated hepatocytes, after incubation in hepatocyte differentiation medium. Non-differentiated (collected on day 4 after cell plating) and differentiated (collected on day 14 after incubation in hepatocyte differentiation medium) MSCs were analyzed using hepatocyte makers, including cytochrome P450 3A4 (CYP3A4) and phosphoenolpyruvate carboxykinase 1 (PCK1), with western blotting (Fig. 2D). The results showed that CYP3A4 and PCK1 expression of hMSC increased in differentiated cells (normalized intensity of CYP3A4 was 2.34 and of PCK1 was 1.89) compared to non-differentiated cells (normalized intensity of CYP3A4 was 1.00 and of PCK1 was 1.00). Similar results were obtained for the mMSC group, with CYP3A4 and PCK1 expression increasing in differentiated cells (normalized intensity of CYP3A4 was 1.99 and of PCK1 was 1.80) compared to non-differentiated cells (normalized intensity of CYP3A4 was 1.00 and of PCK1 was 1.00). hMSCs and mMSCs showed similar differentiation potency.

Mouse MSCs Reduced the Area of Liver Injury Better than Human MSCs in Mice with CCl₄-Induced Acute Liver Failure

Carbon tetrachloride is the most common material used to induce acute liver failure in animal models. The cytochrome P450 family of enzymes metabolize carbon tetrachloride into the trichloromethyl radical, which has high reactivity for destroying nucleic acids, proteins, and lipids in hepatocytes leading to acute liver failure.¹⁷ The disease pathology is similar to that of drug-induced acute liver failure in humans, such as acetaminophen.¹⁸ Therefore, this model is a suitable approach to designing therapeutic strategies against reactive metabolite-induced hepatic toxicity. This study evaluated the differences in the efficacy of hMSC and mMSC therapies in the early stage (days 0-3) of CCl₄-induced acute liver failure (Fig. 3A).

Mouse body weight at the end of the MSC treatment (day 3) was not significantly different from that at day 0 (Supplementary Fig. S2A). Serum alanine transaminase (ALT) and aspartate transaminase (AST) biochemistry values indicate the level of liver injury. The ALT (Fig. 3B) and AST (Fig. 3C) values were significantly lower in CCl₄/hMSC (ALT: 1056 U/L; AST: 480 U/L) and CCl₄/mMSC (ALT: 1021 U/L; AST: 474 U/L) groups compared to the CCl₄ group (ALT: 2397 U/L; AST: 1650 U/L) of immunocompetent mice with CCl₄-induced

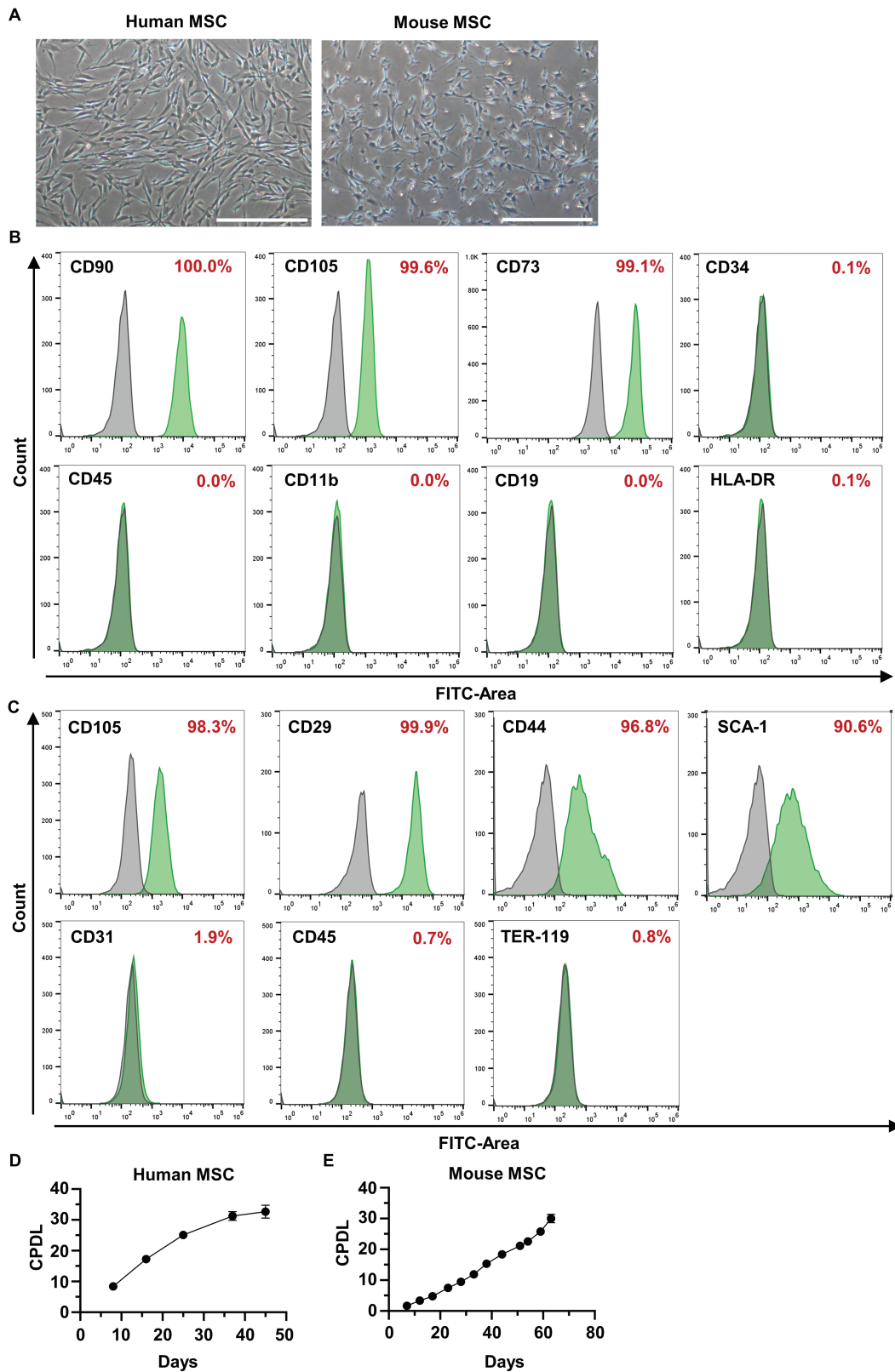


Figure 1. Characterization of human and mouse adipose-derived mesenchymal stem cell (MSC) morphology, MSC markers, and cell population doubling level (CPDL). **(A)** Human and mouse adipose-derived MSCs showed spindle cell morphology. Scale bar: 250 μ m. **(B)** Evaluation of hMSC markers by fluorescence-activated cell sorting (FACS). **(C)** Evaluation of mMSC markers by FACS. **(D)** The cell-doubling time of human MSCs was analyzed using the cell population doubling level (CPDL). Data are shown in mean \pm SD; $n = 3$ independent experiments. **(E)** The cell-doubling time of mouse MSCs was analyzed using CPDL. Data are represented as mean \pm SD; $n = 3$ independent experiments. See also [Supplementary Fig. S1](#).

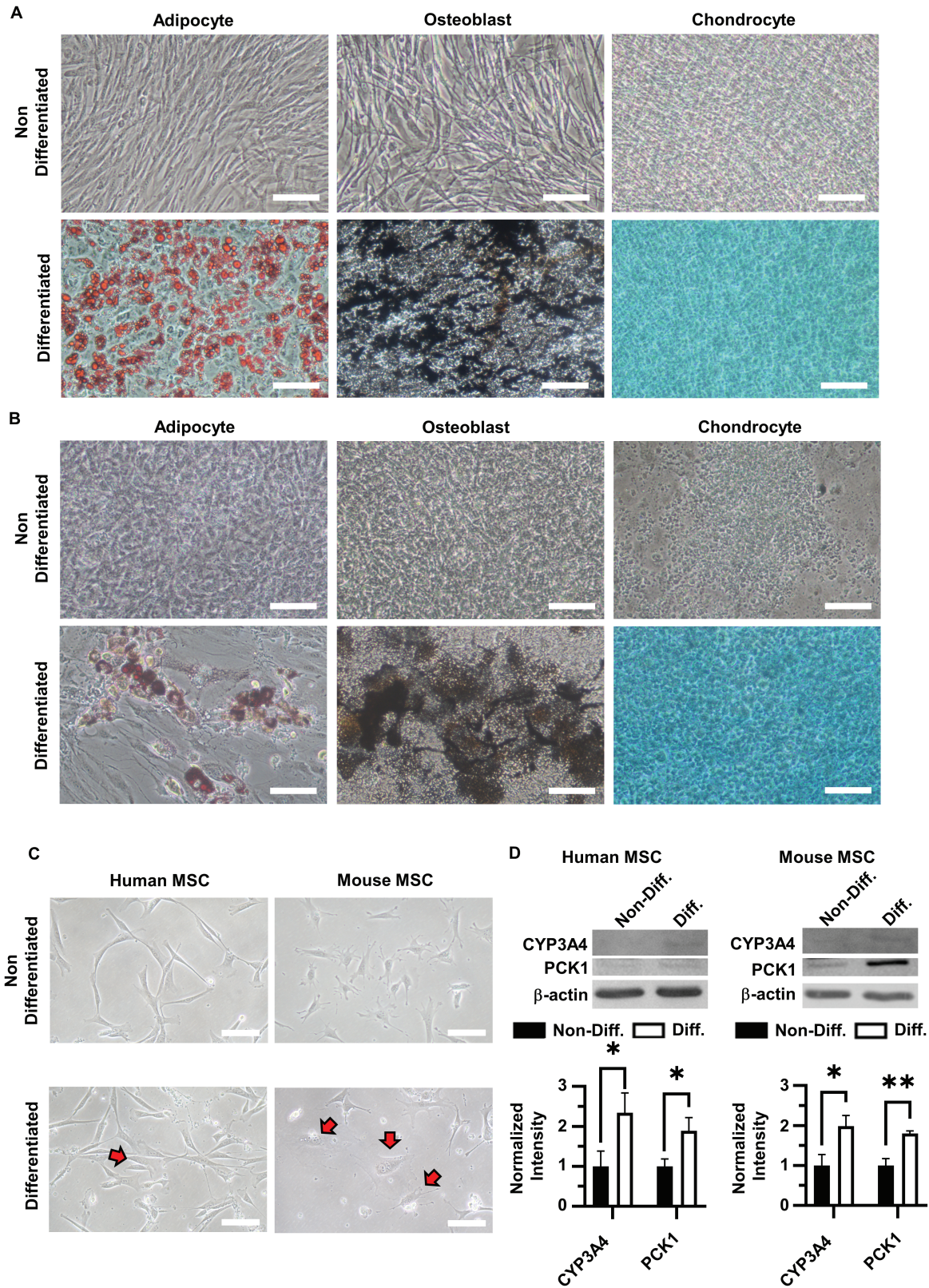


Figure 2. Human and mouse mesenchymal stem cells (MSCs) have the potency to differentiate into adipocytes, osteoblasts, chondrocytes, and hepatocytes. **(A)** Human MSCs (hMSCs) differentiated into adipocytes, osteoblasts, and chondrocytes. Scale bar: 100 μ m. **(B)** Mouse MSCs (mMSCs) differentiated into adipocytes, osteoblasts, and chondrocytes. Scale bar: 100 μ m. **(C)** The hMSCs and mMSCs differentiating into hepatocytes showed polyploidization morphology. The arrows indicate binucleated hepatocytes. Scale bar: 100 μ m. **(D)** The differentiated hMSCs and mMSCs in (C) were evaluated for hepatocyte-related CYP3A4 and PCK1 protein expression by western blot. β -actin was the loading control. The CYP3A4 and PCK1 quantification results were normalized using the non-Diff group; data are shown in mean \pm SD; $n = 3$ independent experiments. Unpaired t -test (compared to non-diff): $P < .05$ (*), $< .01$ (**), $< .001$ (***), $< .0001$ (****). Abbreviations: non-Diff, non-differentiated cell; Diff., differentiated cell.

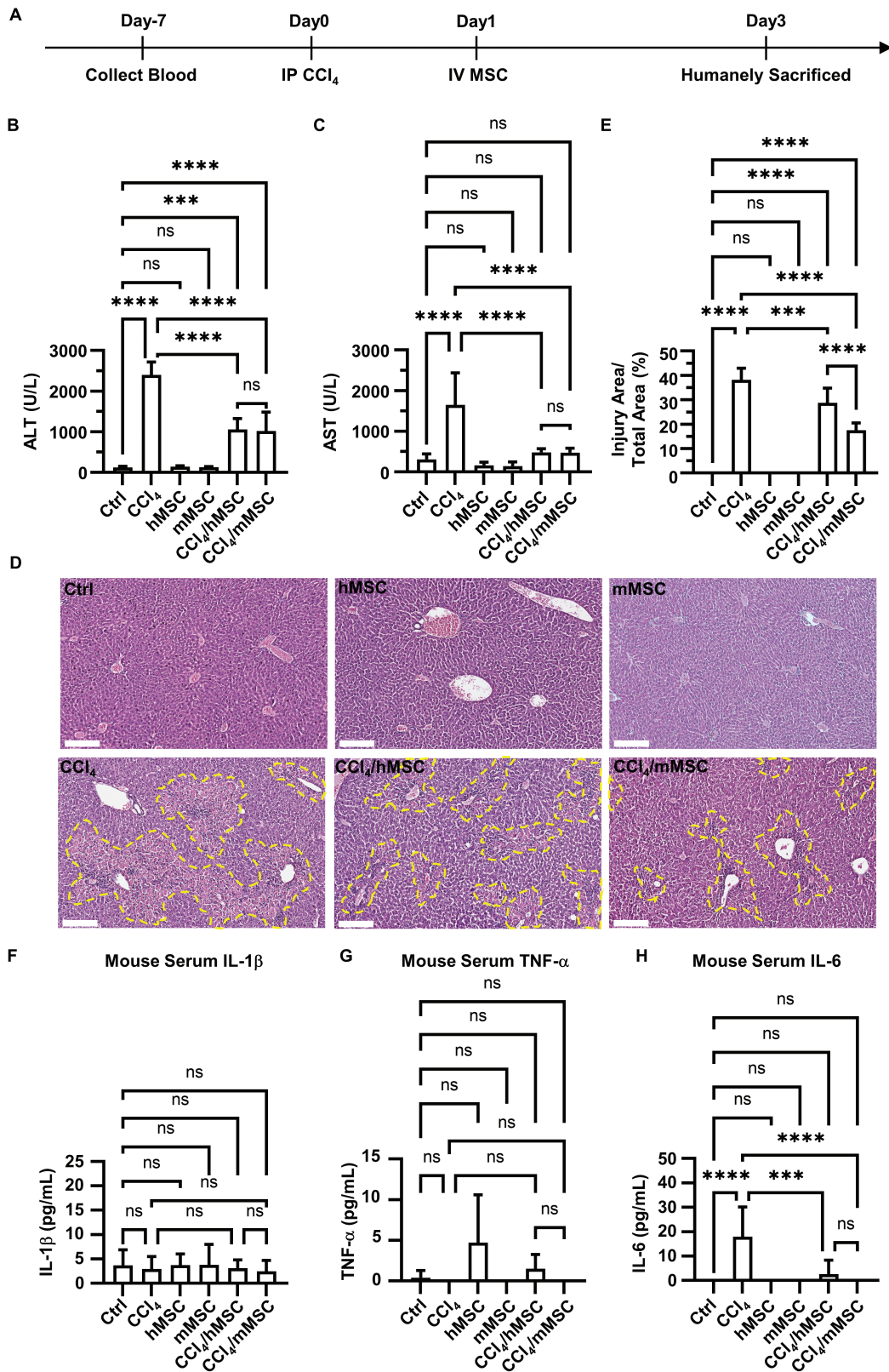


Figure 3. Both human and mouse MSC therapies reduced liver injury biochemistry values and systemic pro-inflammatory cytokine IL-6 in mice with early-stage acute liver failure. **(A)** Schematic diagram of CCl₄-induced acute liver failure and hMSC and mMSC therapy. **(B)** Serum concentration of ALT (serum glutamic pyruvic transaminase, sGPT) and **(C)** AST (serum glutamic-oxaloacetic transaminase, sGOT) of mice with liver failure at day 3. Data are shown in mean ± SD; n = 5-8 animals; one-way ANOVA: *P* < .05(*), < .01(**), < .001(***) , < .0001(****). **(D)** Mouse liver sections stained with H&E at day 3. Scale bar: 200 μm. **(E)** Quantification of the area of liver injury in **(D)**. The injured results were normalized by the total area. Data are shown in mean ± SD; n = 5-8 independent experiments; one-way ANOVA: *P* < .05(*), < .01(**), < .001(***) , < .0001(****). **(F-H)** Expression of blood IL-1β (**F**), TNF-α (**G**), and IL-6 (**H**) concentration at day 3 in mice with acute liver failure. Data are shown in mean ± SD; n = 5-8 animals; one-way ANOVA: *P* < .05(*), < .01(**), < .001(***) , < .0001(****). See also [Supplementary Fig. S2](#).

liver failure. The hMSC and mMSC groups did not show any liver toxicity. In the CCl₄-damaged liver, reactive metabolites bind to lipids and proteins to influence lipoprotein and calcium homeostasis leading to an increase in liver mass.¹⁹ The organ to body weight percentages were analyzed at day 3 of the study (Supplementary Fig. S2B-K). The liver/body weight percentage decreased in the CCl₄/hMSC (6.92%) and CCl₄/mMSC (6.71%) groups, which approached the healthy control group (6.42%), compared to the CCl₄ group (7.88%) of immunocompetent mice with CCl₄-induced liver failure (Supplementary Fig. S2D). The liver-damaged regions were visualized by histological H&E staining. The areas of the damaged liver showed a loss of hepatocyte nuclei and were more pinkish in color (Fig. 3D). The damaged area of the liver was also quantified as a percentage (Fig. 3E). Strikingly, the CCl₄/mMSC group had the smallest injured area by percentage (17.50%) compared to the CCl₄ (38.16%) and CCl₄/hMSC (28.77%) groups. The differences in the extent of liver damage of immunocompetent mice with acute liver failure given hMSC and mMSC therapies indicate that the therapeutic mechanisms of these MSCs should be evaluated.

Acute liver failure arouses a systemic inflammatory response that is altered by macrophage-derived pro-inflammatory cytokines, including interleukin-1 (IL-1), tumor necrosis factor- α (TNF- α), and IL-6.²⁰⁻²² The serum IL-1 β , TNF- α , and IL-6 concentrations of mice with acute liver failure were investigated (Fig. 3F-H). The serum IL-1 β and TNF- α concentrations were not significantly different between the groups (Fig. 3F, 3G). However, hMSC therapy slightly increased the TNF- α serum concentration in the hMSC (4.73 pg/mL) and CCl₄/hMSC (1.50 pg/mL) groups (Fig. 3G). The serum IL-6 concentration was significantly lower in the CCl₄/hMSC (2.56 pg/mL) and CCl₄/mMSC (0 pg/mL) groups compared to that of the CCl₄ group (17.93 pg/mL), which indicated that both treatments reduced systemic inflammation (Fig. 3H).

Mouse MSC Therapy Enhanced Liver Regeneration by Increasing Activation of IL-6 and Hepatic Macrophages in the Liver

To evaluate the enhancement of liver regeneration by hMSC and mMSC therapies, we analyzed the levels of the inflammatory cytokine TNF- α , liver regenerative cytokine IL-6, and scavengers of F4/80⁺ hepatic macrophages in the liver region by immunohistochemistry (IHC) sections. The liver region IHC results showed that TNF- α expression of CCl₄/hMSC (intensity/total area of 0.27) and CCl₄/mMSC (intensity/total area of 2.16) groups were significantly lower than that of the CCl₄ group (intensity/total area of 11.97) (Fig. 4A), indicating that the hMSC and mMSC treatments reduced the inflammation of the damaged liver of immunocompetent mice with liver failure.

Interestingly, the IHC results for the liver showed a significantly increased IL-6 signal in mMSC (intensity/total area of 9.41) and CCl₄/mMSC (intensity/total area of 5.37) groups compared to the control (intensity/total area of 0.47), CCl₄ (intensity/total area of 0.99), hMSC (intensity/total area of 1.45), and CCl₄/hMSC (intensity/total area of 1.43) groups (Fig. 4B). In the CCl₄ group, the IL-6 signal was mainly expressed in the hepatic cells of the damaged region. In contrast, the main IL-6 signals were detected in the cytoplasm of hepatocytes in the mMSC and CCl₄/mMSC groups. These results highlight that the mMSC intervention enhanced

IL-6-dependent liver regeneration in immunocompetent mice more than the hMSC intervention (Fig. 4B, indicated by the arrows).

The F4/80⁺ hepatic macrophages increased in the liver region of the CCl₄ (intensity/total area of 54.08) and CCl₄/mMSC (intensity/total area of 61.43) groups compared to the control (intensity/total area of 12.45), hMSC (intensity/total area of 12.09), mMSC (intensity/total area of 18.16), and CCl₄/hMSC (intensity/total area of 22.12) groups (Fig. 4C). Interestingly, the CCl₄/mMSC group showed higher hepatic macrophage recruitment into the damaged area of the liver than the CCl₄/hMSC group of immunocompetent mice with acute liver failure. However, the F4/80⁺ hepatic macrophages recruited in the CCl₄/mMSC group did not secrete TNF- α . Instead, the abundant F4/80⁺ hepatic macrophages recruited in the CCl₄ group secreted TNF- α (Fig. 4A, 4C, indicated by red arrows).

The TNF- α , IL-6, and F4/80 results showed that the CCl₄ group induced TNF- α secretion by recruiting F4/80⁺ hepatic macrophages. The CCl₄/hMSC group inhibited F4/80⁺ hepatic macrophages recruited into the damaged liver region, thus reducing TNF- α secretion. On the other hand, the CCl₄/mMSC group maintained F4/80⁺ hepatic macrophages recruited into the damaged liver region, reduced TNF- α secretion, and enhanced IL-6-dependent liver regeneration, which resulted in a smaller injury area of liver in the CCl₄/mMSC group than in the CCl₄/hMSC group (Fig. 3E).

Human and Mouse MSC Therapies Reduced Myofibroblast Activation Through Influencing TGF- β 1 Expression in Areas of Liver Injury

TGF- β 1 is a profibrogenic growth factor secreted by F4/80⁺ hepatic macrophages.²³⁻²⁵ Inflammatory F4/80⁺ hepatic macrophages activate hepatic stellate cells (HSCs) and promote their transdifferentiation into myofibroblasts, which express α -smooth muscle actin (α -SMA) during liver restoration.²⁶⁻²⁸ The fibrotic potential of mice with acute liver failure was characterized by TGF- β 1 and α -SMA. The primary TGF- β 1 signal was a secretory type and mostly accumulated in the damaged area of the liver.

The CCl₄/hMSC (intensity/total area of 7.36) and CCl₄/mMSC (intensity/total area of 5.71) groups accumulated less TGF- β 1 in the damaged region of the liver than the CCl₄ group (intensity/total area of 21.36) (Fig. 5A, indicated by red arrows). The α -SMA signal was an intracellular type in HSC-derived myofibroblasts (Fig. 5B, the arrows). The α -SMA IHC results indicated that both MSC interventions reduced the activation of myofibroblasts in damaged regions of the liver (CCl₄/hMSC: intensity/total area of 59.42; CCl₄/mMSC: intensity/total area of 58.36) to a greater extent than the CCl₄ group (intensity/total area of 75.11). According to the TGF- β 1 and α -SMA IHC results, myofibroblast activation was reduced in the CCl₄/hMSC and CCl₄/mMSC groups due to a decrease in TGF- β 1 accumulation in the damaged liver region.

According to hepatic macrophage recruitment (Fig. 4C) and these findings, the CCl₄/hMSC group showed lower TGF- β 1 expression because F4/80⁺ hepatic macrophages were not recruited. The CCl₄/mMSC group maintained F4/80⁺ hepatic macrophage recruitment with lower TGF- β 1 expression and α -SMA⁺ myofibroblast activation, which might have allowed F4/80⁺ hepatic macrophages to turn into restorative hepatic macrophages.²⁹

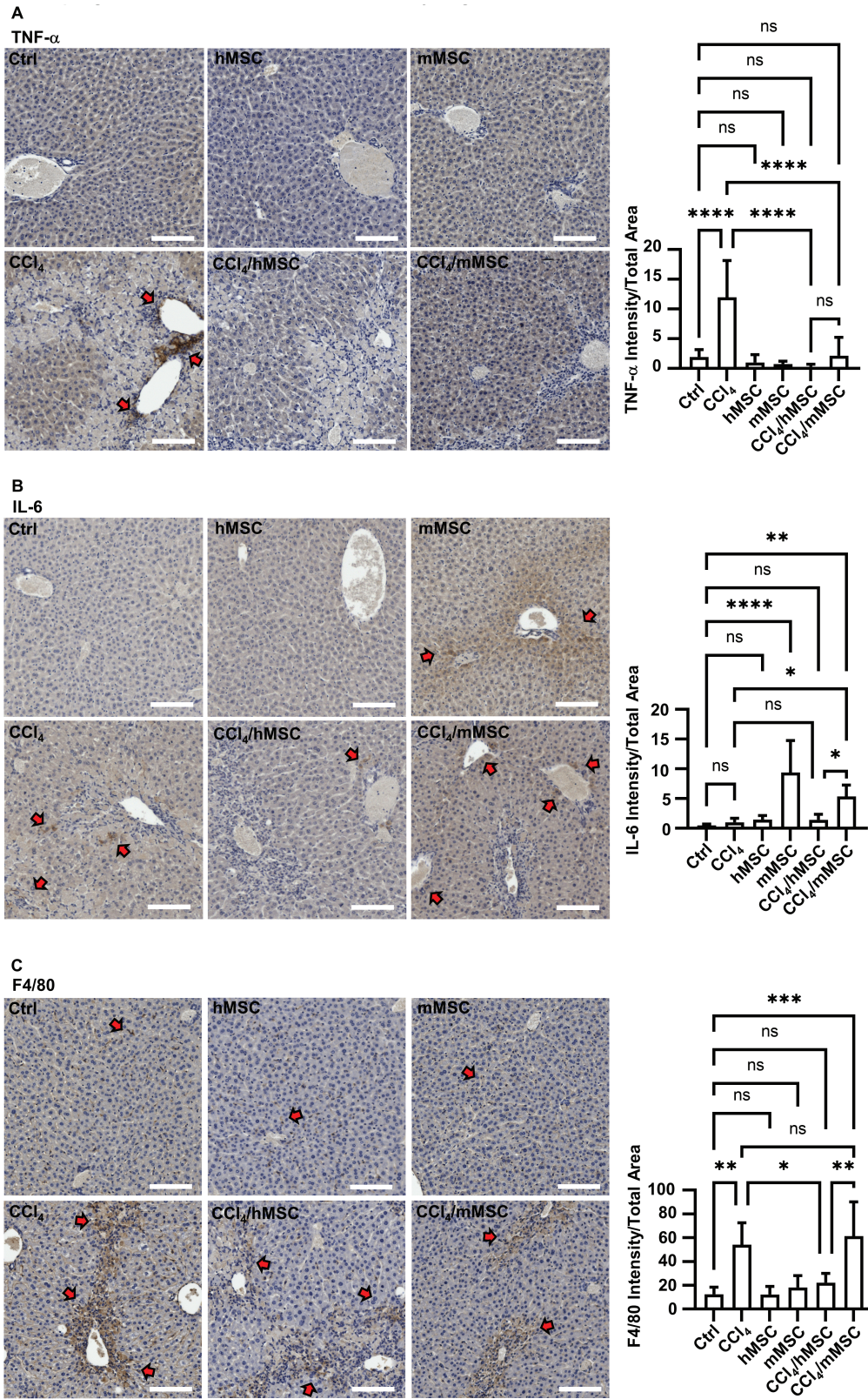


Figure 4. Mouse MSC therapy enhanced liver regeneration by increasing IL-6 and F4/80⁺ hepatic macrophage activation in the liver of mice with early-stage acute liver failure. **(A-C)** Expression of immunohistochemistry (IHC) quantification results of TNF- α (A), IL-6 (B), and F4/80⁺ hepatic macrophages (C) in the liver region. The arrows indicate the positive sites. The results of quantified intensity were normalized by total liver tissue area. Scale bar: 100 μ m; Data are shown in mean \pm SD; $n = 5-8$ independent experiments; one-way ANOVA: $P < .05$ (*), $< .01$ (**), $< .001$ (***), $< .0001$ (****).

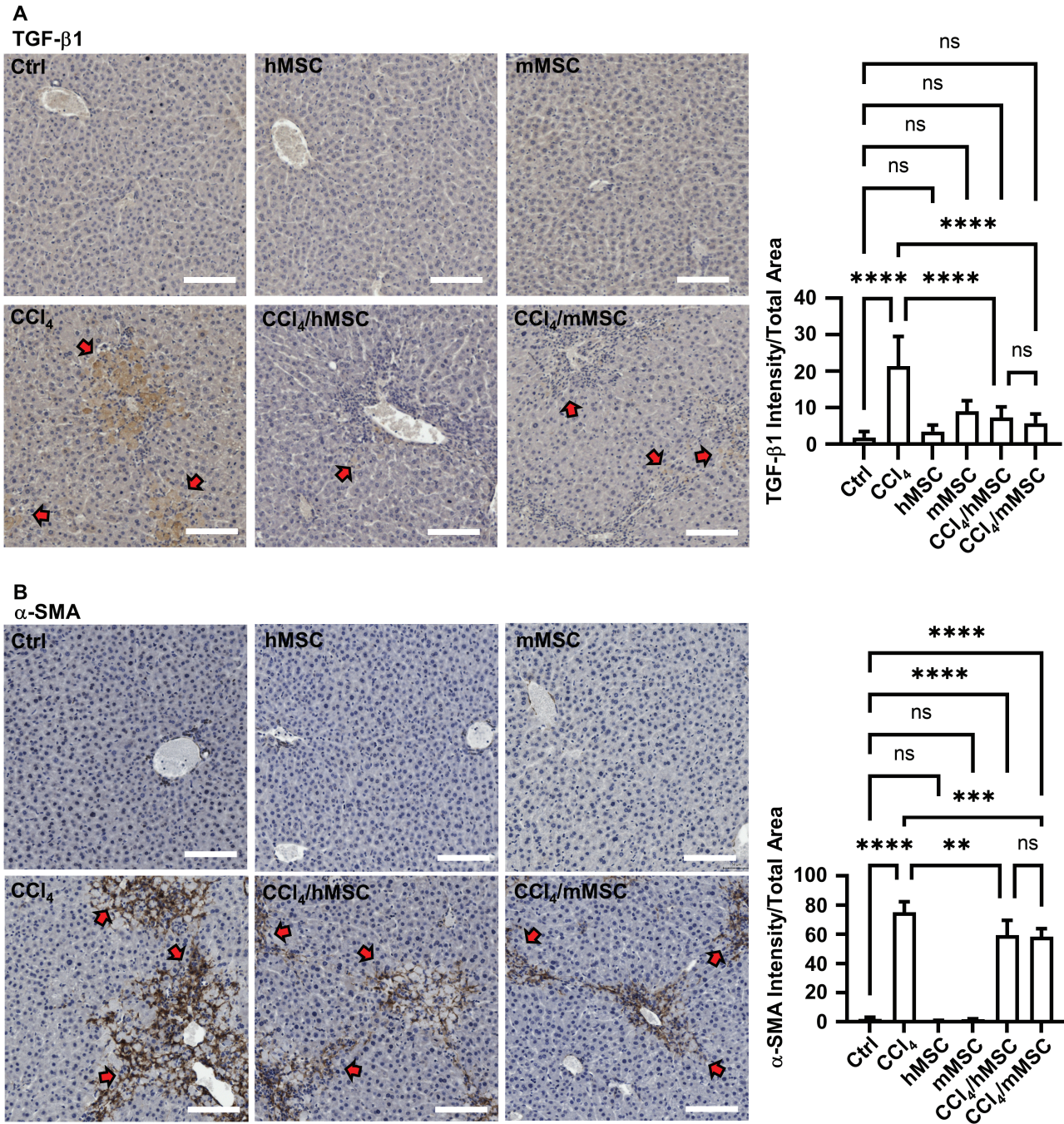


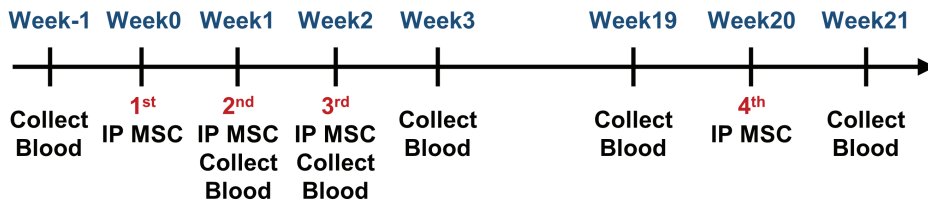
Figure 5. TGF-β1 in the injured region of liver influenced mouse liver fibrosis by myofibroblast activation by human and mouse MSC therapies. **(A, B)** Expression of IHC quantification results of TGF-β1 (A) and α-SMA (B) in the liver region. The arrows indicate the positive sites. The results of quantified intensity were normalized by total liver tissue area. Scale bar: 100 μm; Data are shown in mean ± SD; n = 5-8 independent experiments; one-way ANOVA: P < .05(*), < .01(**), < .001(***), < .0001(****).

Human MSCs Induced an Antibody Immune Response in Immunocompetent Mice

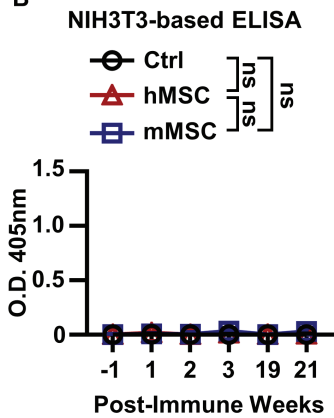
MSCs secrete immunomodulatory factors, including TGF-β1, prostaglandin E2 (PEG2), and TNF-stimulated gene 6 (TSG-6) protein, to evade phagocytosis by antigen-presenting cells (APCs) and T lymphocyte cell cytotoxicity.³⁰ However, xenotransplantation can cause a stronger immune response than allotransplantation.³¹ Therefore, to confirm the hypothesis, hMSCs and mMSCs were injected into immunocompetent mice to evaluate the antibody immune response (Fig. 6A). The immunocompetent mice and mMSC were from the identical

inbred generation of C57BL/6 mice to avoid the allograft transplantation immune response.^{32,33} To analyze hMSC and mMSC immune responses, we generated mouse fibroblast (NIH3T3)-, hMSC-, and mMSC-based ELISA to detect anti-hMSC or anti-mMSC antibodies in mouse serum. The NIH3T3 cell-based ELISA excluded the non-specific mouse antibodies (Fig. 6B). ELISA results showed that the hMSC group had a significant anti-hMSC antibody signal at week 2. After the hMSC boost, the hMSC group showed a stronger anti-hMSC antibody signal at week 21 (O.D. = 0.95) than at weeks 2 (O.D. = 0.46) and 3 (O.D. = 0.65) (Fig. 6C). Instead,

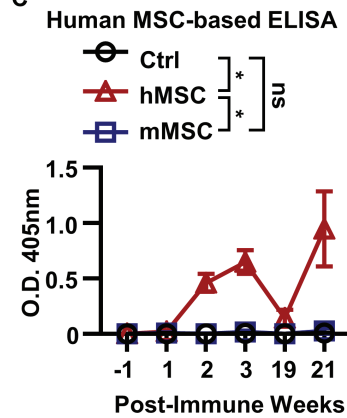
A



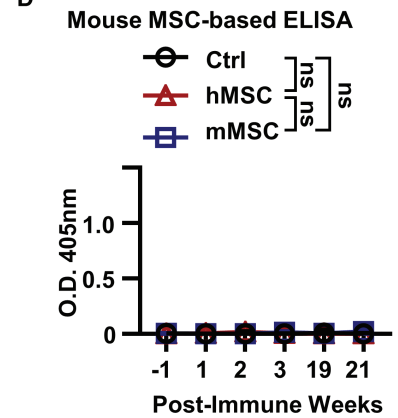
B



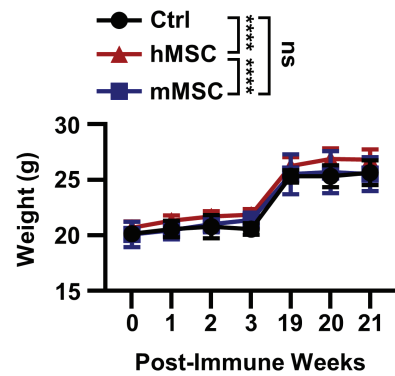
C



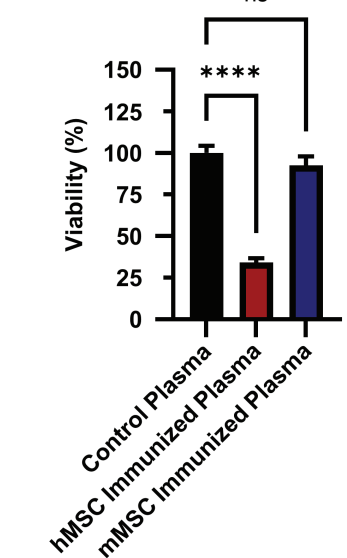
D



E



F



G

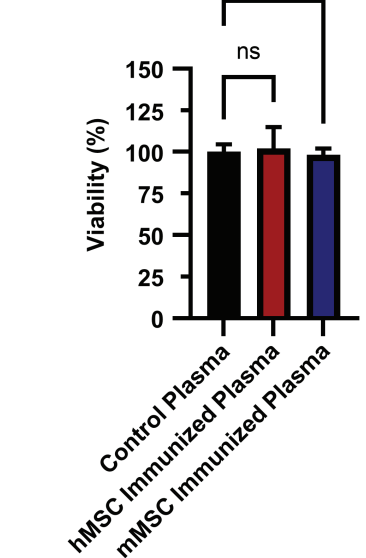


Figure 6. Human MSC therapy induced an antibody immune response in mice given long-term MSC therapy. (A) Schematic diagram of long-term human and mouse MSC therapies for C57BL/6 mice. (B-D) Expression of (B) NIH3T3 (mouse fibroblast) cell-based ELISA for excluding non-specific serum antibody binding, (C) hMSC-based ELISA for evaluating serum anti-hMSC antibodies, and (D) mMSC-based ELISA for investigating serum anti-mMSC antibodies. Data are shown in mean \pm SD; $n = 5$ animals; one-way ANOVA (repeated measures): $P < .05$ (*), $< .01$ (**), $< .001$ (***), $< .0001$ (****). (E) Mouse body weight. Data are shown in mean \pm SD; $n = 5$ animals; one-way ANOVA (repeated measures): $P < .05$ (*), $< .01$ (**), $< .001$ (***), $< .0001$ (****). (F, G) hMSC and mMSC viability in mouse plasma. (F) hMSCs were treated with control plasma, hMSC-immunized plasma, and mMSC-immunized plasma. Viability values were normalized according to the control plasma. (G) mMSCs were treated with control plasma, hMSC-immunized plasma, and mMSC-immunized plasma. The viability values were normalized according to the control plasma. Data are shown as mean \pm SD; $n = 2-3$ independent experiments; one-way ANOVA (comparing to control mouse plasma): $P < .05$ (*), $< .01$ (**), $< .001$ (***), $< .0001$ (****).

the mMSC-based ELISA results did not show anti-mMSC antibody signals at weeks 2, 3, and 21 (Fig. 6D). No mice showed significant apparent toxicity, but the hMSC group showed body weight gained (Fig. 6E). Next, we evaluated whether immunized mouse plasma affected hMSC and mMSC viability. The results showed that hMSC-immunized plasma significantly decreased hMSC viability (34.2%) compared to control plasma (100%) and mMSC-immunized plasma (92.4%) (Fig. 6F). In contrast, mMSC-immunized plasma did not affect mMSC viability (98.2%) compared to control plasma (100%) and hMSC-immunized plasma (102.1%) (Fig. 6G). This evidence suggests that hMSC transplantation in immunocompetent mice is not an appropriate model for long-term MSC studies because the strong anti-hMSC antibody responses decrease hMSC viability.

Discussion

The hMSC and mMSC therapies demonstrated diverse therapeutic mechanisms in immunocompetent mice with CCl₄-induced acute liver failure. Both hMSCs and mMSCs showed potency to differentiate into hepatocyte-like cells and reduced ALT and AST concentrations in blood. Interestingly, the damaged area of the liver in the CCl₄/mMSC group (17.50%) was significantly less than that in the CCl₄/hMSC (28.77%) group, which indicates that xenograft and allograft MSC transplantations affected the therapy results. Furthermore, our findings showed that both the CCl₄/hMSC and CCl₄/mMSC groups had lower IL-6 concentrations in blood, which reduced systemic inflammation. In the CCl₄/mMSC group, mMSCs reduced TNF- α secretion, enhanced IL-6-dependent liver cell proliferation, and induced F4/80⁺ hepatic macrophage recruitment to the damaged area of the liver, which benefited liver regeneration. However, in the CCl₄/hMSC group, hMSC therapy only lowered TNF- α secretion by reducing F4/80⁺ hepatic macrophage recruitment. In the case of activation of fibrosis, the CCl₄/hMSC and CCl₄/mMSC groups both showed lower pro-fibrotic TGF- β 1 secretion and myofibroblast activation in the damaged liver. Finally, we demonstrated that hMSCs, rather than mMSCs, significantly induced an antibody immune response in the immunocompetent mice, and are, consequently, inappropriate for long-term study.

Liver regeneration activates abundant intracellular and extracellular signals in F4/80⁺ hepatic macrophages and hepatocytes, including complete mitogens (HGF and EGFR ligands) and auxiliary mitogens (IL-6 and TNFs).² The F4/80⁺ hepatic macrophages are the leading surveillance and scavenger cells to sense and remove danger-associated molecular patterns (DAMPs) during acute liver failure.³⁴ The activation of hepatic macrophages increases the secretion of the M1 phenotype of inflammasome factors, including TNF- α , and IL-6, and later induces the secretion of the M2 restorative phenotype of anti-inflammatory cytokines, including IL-10, to improve liver regeneration and reduce inflammation. TNF- α upregulates NF- κ B, leading to higher pro-inflammatory cytokine secretion in F4/80⁺ hepatic macrophages.¹ However, TNF- α also recruits more hepatic and monocyte-derived macrophages, leading to an acute inflammatory response.³⁵ In a previous study on mouse MSC acute liver failure, mouse MSC treatment reduced TNF- α gene expression in the damaged mouse liver region where paracrine prostaglandin E2 (PGE2) in MSCs downregulated hepatic macrophage

TGF- β -activated kinase 1 (TAK1) signaling and NLRP3 (NOD-, LRR- and pyrin domain-containing protein 3) inflammasome activation to reduce hepatic macrophage inflammatory cytokine secretion and induce M2 macrophage polarization.³⁶ Another study showed allogeneic MSC immunomodulatory effects in human MSC cocultured *ex vivo* with human macrophages; MSC-secreted paracrine reduced the inflammatory response of macrophages, which in turn reduced TNF- α inflammatory cytokine concentration.³⁷ According to these studies, MSCs are regarded as reducing TNF- α in the damaged liver region by decreasing the inflammatory response of hepatic macrophages. Nevertheless, the reduced activation of hepatic macrophages may also decrease hepatic macrophage-related liver regeneration, including IL-6-dependent liver proliferation and DAMP phagocytosis. The lack of IL-6 impairs liver regeneration in IL-6 knockout mice.³⁸ In addition, mice subjected to partial hepatectomy show increased liver cell proliferation with recombinant IL-6 and hyper-IL-6 therapies.³⁹ IL-6-regulated signal transducer and activator of transcription 3 (STAT3) intracellular signals are related to liver regeneration.⁴⁰ Moreover, IL-6 expression in hepatocytes is correlated with HGF/MET-dependent hepatocyte proliferation.⁴¹ These studies indicate that IL-6 is a crucial factor in liver regeneration. Our findings show that both CCl₄/hMSC and CCl₄/mMSC groups had reduced TNF- α expression in the damaged region of the liver of immunocompetent mice with acute liver failure. IL-6 expression was evident in only the CCl₄/mMSC group, which indicated that hepatocyte regeneration in this group was better than that in the CCl₄/hMSC group. Furthermore, the CCl₄/mMSC group showed increased recruitment of F4/80⁺ hepatic macrophages in the damaged area of the liver, which enhanced the likelihood of clearance of DAMPs. According to these results, IL-6-dependent liver proliferation and F4/80⁺ hepatic macrophage activation were maintained in the CCl₄/mMSC group in contrast to the CCl₄/hMSC group. These findings explain why the extent of liver damage in the CCl₄/mMSC group was less than that in the CCl₄/hMSC group.

In addition to contributing to liver regeneration with DAMP phagocytosis and auxiliary mitogen secretion, F4/80⁺ hepatic macrophages also secrete TGF- β 1, which has been reported to have hepatocyte mitoinhibitory properties and induce liver fibrosis.^{2,34} TGF- β 1 causes hepatic satellite cells (HSCs) to differentiate into α -SMA⁺ myofibroblasts.⁴² The continuous activation of α -SMA⁺ myofibroblasts leads to extracellular matrix (ECM) accumulation and fibrosis. Truong's study demonstrated that allogeneic mouse MSC treatment reduced TGF- β gene expression in the injured mouse liver region.⁴³ Khalifa's study also found that allogeneic rat MSC treatment reduced TGF- β gene expression in injured rat liver.⁴⁴ Moreover, Ramachandran's study described the different functions of the F4/80⁺/Ly6C^{hi} inflammatory and F4/80⁺/Ly6C^{lo} restorative hepatic macrophage subsets. The F4/80⁺/Ly6C^{hi} hepatic macrophages express genes for inflammatory cytokines (TNF- α , etc.), pro-fibrotic growth factors (TGF- β 1, etc.), and chemokines. The F4/80⁺/Ly6C^{lo} hepatic macrophages express genes for matrix degradation and phagocytosis.⁴⁵ Li's study showed that allogeneic mouse bone marrow-MSC (BM-MSC) modulated the F4/80⁺/Ly6C^{hi} and F4/80⁺/Ly6C^{lo} ratio in a mouse CCl₄-chronic liver injury model. BM-MSC reduced the population of F4/80⁺/Ly6C^{hi} hepatic macrophages (ie, decreased TNF- α and TGF- β 1 expression)

and increased the F4/80⁺/Ly6C^{lo} population, further reducing liver fibrosis.²⁹ According to these studies, TGF- β 1 is the critical factor of liver myofibroblast activation and MSC's immunomodulatory effects that reduced liver fibrosis by modulating the inflammatory and restorative hepatic macrophage population. We found that the hMSC and mMSC therapies had different mechanisms for reducing TGF- β 1 expression and α -SMA⁺ myofibroblast activation in the damaged region of the liver. TGF- β 1 profibrotic factor accumulation of the CCl₄/hMSC group was lower due to reduced F4/80⁺ hepatic macrophage infiltration into the damaged area of the liver. In contrast, the CCl₄/mMSC group had a different ability to maintain the infiltration of F4/80⁺ hepatic macrophages into the damaged liver and their lower secretion of the TGF- β 1 profibrotic factor.

The MSC-related immunomodulatory factors have greater applicability to transplantation than other cell therapies. However, according to,³⁰ MSCs are immune-evasive but not immune-privileged. Even if hMSCs can escape the immune response, xenotransplantation leads to an immune response in T-cell-deficient mice.¹⁰ Therefore, immunodeficient mice are the standard model for human MSC studies. In our study, hMSCs showed an anti-human MSC antibody response starting at week 2, indicating that hMSC therapy is unsuitable for long-term treatment studies of immunocompetent mice. Notably, mMSCs did not show an antibody response in immunocompetent mice, indicating that mMSC therapy is suitable for long-term treatment studies.

High concentrations of pro-inflammatory cytokines, including TNF- α and IL-6, are usually detected in the blood of acute liver failure patients, indicating systemic inflammation.^{21,46} Systemic macrophage-secreted pro-inflammatory cytokines, including IL-1, TNF, and IL-6, and proteolytic enzymes, reactive oxygen species, and lysosomal enzymes increased the risk of aggravation of encephalopathy in patients with acetaminophen-induced acute liver failure.^{20,47} In mice with lipopolysaccharide (LPS)-induced systemic inflammation, MSC-mediated treatment is reported to reduce blood TNF- α and systemic inflammation.⁴⁸ MSCs have also been investigated for their immunomodulatory effects and benefits for acute graft-versus-host disease (GvHD) patients.⁴⁹ Our findings demonstrated that both CCl₄/hMSC and CCl₄/mMSC groups had reduced systemic IL-6 concentrations in blood. Nevertheless, hMSCs slightly induced TNF- α (pro-inflammatory cytokine) concentration in the blood of immunocompetent mice, which might be a xenotransplantation-induced innate immune response.⁵⁰ The blood TNF- α result confirms that hMSCs are unsuitable for studying therapeutic mechanisms in immunocompetent mice with acute liver failure.

Conclusion

Our study shows that mMSCs are more suitable than hMSCs for studying acute liver failure in immunocompetent mice. The mMSC therapy recruited liver regeneration-related F4/80⁺ hepatic macrophages to the damaged region of the liver, increased IL-6 expression in hepatocytes to enhance further hepatocyte proliferation, and reduced TNF- α secretion in the liver of immunocompetent mice with acute liver failure. Moreover, mMSC therapy reduced α -SMA⁺ myofibroblast activation by decreasing TGF- β 1 accumulation in the injured areas of the liver, which decreased the likelihood of liver

fibrosis. In contrast, the hMSC therapy did not show F4/80⁺ hepatic macrophage recruitment to the damaged parts of the liver. Although the hMSC therapy reduced TNF- α -related inflammation and TGF- β 1-related fibrosis, it also led to the loss of potency of F4/80⁺ hepatic macrophages to remove damaged hepatocytes and promote IL-6-dependent liver regeneration. Therefore, mMSCs have better therapeutic efficacy than hMSCs in immunocompetent mice with acute liver injury. Finally, because of its immunogenicity, the results demonstrate that hMSC therapy is not suitable for long-term exploration of immunomodulatory effects in immunocompetent mice. This comparative study of hMSCs and mMSCs provides reference information for further MSC studies of immunocompetent mice.

Acknowledgments

We would like to acknowledge the Taiwan Mouse Clinic, Academia Sinica, and Taiwan Animal Consortium for technical support in H&E and IHC slides scanning. We thank National Laboratory Animal Center (NLAC), NARLabs, Taiwan, and Taipei Medical University Laboratory Animal Center, Taiwan, for high-quality animals and great animal care. The Taiwan Taipei Medical University core facility faculty members, Yeh-Lin Lu and Ting-Hao Wang, for their excellent technical support in using the SONY SA3800 spectral flow cytometer and TissueGnostics Axio Observer Z1 microscope.

Funding

This work was supported by grants from the National Science and Technology Council, Taiwan (NSC 111-2628-B-038-024, NSC 111-2320-B-038-071, NSC 111-2314-B-075A-014); the National Health Research Institutes, Taiwan (NHRI-EX111-10935SI); and the Ministry of Education, Taiwan.

Conflict of Interest

The authors declare no competing interests to influence the results in this study.

Author Contributions

C.-H.W.: performed most of the experiments and wrote most of the manuscript. K.-H.W. and A.-P.K.: provided MSC isolation and cell culturing advice. C.-H.W. and A.-P.K.: conducted the hMSC and mMSC isolation, cell culture, and cell analysis studies. C.-H.W., C.-Y.C., Y.-J.C., P.-H.L., M.C., and T.-Y.W.: contributed to the animal experiments. C.-Y.C.: contributed the IHC experiments. K.-H.C., J.-J.C., and K.-D.L.: supervised the whole study. K.-H.C.: acquired the funding and provided manuscript writing advice.

Data Availability

The datasets in this study are available from the corresponding authors.

Supplementary Material

Supplementary material is available at *Stem Cells Translational Medicine* online.

References

1. Fausto N, Campbell JS, Riehle KJ. Liver regeneration. *Hepatology*. 2006;43(2 Suppl 1):S45-S53. <https://doi.org/10.1002/hep.20969>
2. Michalopoulos GK, Bhushan B. Liver regeneration: biological and pathological mechanisms and implications. *Nat Rev Gastroenterol Hepatol*. 2021;18(1):40-55. <https://doi.org/10.1038/s41575-020-0342-4>
3. Forbes SJ, Newsome PN. Liver regeneration - mechanisms and models to clinical application. *Nat Rev Gastroenterol Hepatol*. 2016;13(8):473-485. <https://doi.org/10.1038/nrgastro.2016.97>
4. Brenner C, Galluzzi L, Kepp O, Kroemer G. Decoding cell death signals in liver inflammation. *J Hepatol*. 2013;59(3):583-594. <https://doi.org/10.1016/j.jhep.2013.03.033>
5. Zhang Z, Wang FS. Stem cell therapies for liver failure and cirrhosis. *J Hepatol*. 2013;59(1):183-185. <https://doi.org/10.1016/j.jhep.2013.01.018>
6. François M, Romieu-Mourez R, Li M, Galipeau J. Human MSC suppression correlates with cytokine induction of indoleamine 2,3-dioxygenase and bystander M2 macrophage differentiation. *Mol Ther*. 2012;20(1):187-195. <https://doi.org/10.1038/mt.2011.189>
7. Alfaifi M, Eom YW, Newsome PN, Baik SK. Mesenchymal stromal cell therapy for liver diseases. *J Hepatol*. 2018;68(6):1272-1285. <https://doi.org/10.1016/j.jhep.2018.01.030>
8. Yang X, Meng Y, Han Z, et al. Mesenchymal stem cell therapy for liver disease: full of chances and challenges. *Cell Biosci*. 2020;10(1):123. <https://doi.org/10.1186/s13578-020-00480-6>
9. Song N, Scholtmeijer M, Shah K. Mesenchymal stem cell immunomodulation: mechanisms and therapeutic potential. *Trends Pharmacol Sci*. 2020;41(9):653-664. <https://doi.org/10.1016/j.tips.2020.06.009>
10. Tee BC, Sun Z. Xenogeneic mesenchymal stem cell transplantation for mandibular defect regeneration. *Xenotransplantation*. 2020;27(5):e12625. <https://doi.org/10.1111/xen.12625>
11. Kruse PFJ. *Tissue Culture: Methods and Applications*. Elsevier Science; 2012.
12. Stock P, Bruckner S, Ebensing S, et al. The generation of hepatocytes from mesenchymal stem cells and engraftment into murine liver. *Nat Protoc*. 2010;5(4):617-627. <https://doi.org/10.1038/nprot.2010.7>
13. Dominici M, Le Blanc K, Mueller I, et al. Minimal criteria for defining multipotent mesenchymal stromal cells. The International Society for Cellular Therapy position statement. *Cytotherapy*. 2006;8(4):315-317. <https://doi.org/10.1080/14653240600855905>
14. El Agha E, Kramann R, Schneider RK, et al. Mesenchymal stem cells in fibrotic disease. *Cell Stem Cell*. 2017;21(2):166-177. <https://doi.org/10.1016/j.stem.2017.07.011>
15. Lee KD, Kuo TK, Whang-Peng J, et al. In vitro hepatic differentiation of human mesenchymal stem cells. *Hepatology*. 2004;40(6):1275-1284. <https://doi.org/10.1002/hep.20469>
16. Yin L, Zhu Y, Yang J, et al. Adipose tissue-derived mesenchymal stem cells differentiated into hepatocyte-like cells in vivo and in vitro. *Mol Med Rep*. 2015;11(3):1722-1732. <https://doi.org/10.3892/mmr.2014.2935>
17. Scholten D, Trebicka J, Liedtke C, Weiskirchen R. The carbon tetrachloride model in mice. *Lab Anim*. 2015;49(1 Suppl):4-11. <https://doi.org/10.1177/0023677215571192>
18. Yuan L, Kaplowitz N. Mechanisms of drug-induced liver injury. *Clin Liver Dis*. 2013;17(4):507-5518. <https://doi.org/10.1016/j.cld.2013.07.002>
19. Ullah H, Khan A, Baig MW, et al. Poncirin attenuates CCL4-induced liver injury through inhibition of oxidative stress and inflammatory cytokines in mice. *BMC Complement Med Ther*. 2020;20(1):115. <https://doi.org/10.1186/s12906-020-02906-7>
20. Rolando N, Wade J, Davalos M, et al. The systemic inflammatory response syndrome in acute liver failure. *Hepatology*. 2000;32(4 Pt 1):734-739. <https://doi.org/10.1053/jhep.2000.17687>
21. Rutherford AE, Hynan LS, Borges CB, et al; ALF Study Group. Serum apoptosis markers in acute liver failure: a pilot study. *Clin Gastroenterol Hepatol*. 2007;5(12):1477-1483. <https://doi.org/10.1016/j.cgh.2007.08.007>
22. Koyama Y, Brenner DA. Liver inflammation and fibrosis. *J Clin Invest*. 2017;127(1):55-64. <https://doi.org/10.1172/JCI88881>
23. Baeck C, Wehr A, Karlmark KR, et al. Pharmacological inhibition of the chemokine CCL2 (MCP-1) diminishes liver macrophage infiltration and steatohepatitis in chronic hepatic injury. *Gut*. 2012;61(3):416-426. <https://doi.org/10.1136/gutjnl-2011-300304>
24. Karlmark KR, Weiskirchen R, Zimmermann HW, et al. Hepatic recruitment of the inflammatory Gr1+ monocyte subset upon liver injury promotes hepatic fibrosis. *Hepatology*. 2009;50(1):261-274. <https://doi.org/10.1002/hep.22950>
25. Seki E, De Minicis S, Osterreicher CH, et al. TLR4 enhances TGF-beta signaling and hepatic fibrosis. *Nat Med*. 2007;13(11):1324-1332. <https://doi.org/10.1038/nm1663>
26. Kisseleva T. The origin of fibrogenic myofibroblasts in fibrotic liver. *Hepatology (Baltimore, Md)*. 2017;65(3):1039-1043. <https://doi.org/10.1002/hep.28948>
27. Tsuchida T, Friedman SL. Mechanisms of hepatic stellate cell activation. *Nat Rev Gastroenterol Hepatol*. 2017;14(7):397-411. <https://doi.org/10.1038/nrgastro.2017.38>
28. Pradere JP, Kluwe J, De Minicis S, et al. Hepatic macrophages but not dendritic cells contribute to liver fibrosis by promoting the survival of activated hepatic stellate cells in mice. *Hepatology*. 2013;58(4):1461-1473. <https://doi.org/10.1002/hep.26429>
29. Li YH, Shen S, Shao T, et al. Mesenchymal stem cells attenuate liver fibrosis by targeting Ly6C(hi/lo) macrophages through activating the cytokine-paracrine and apoptotic pathways. *Cell Death Discov*. 2021;7(1):239. <https://doi.org/10.1038/s41420-021-00584-z>
30. Ankrum JA, Ong JF, Karp JM. Mesenchymal stem cells: immune evasive, not immune privileged. *Nat Biotechnol*. 2014;32(3):252-260. <https://doi.org/10.1038/nbt.2816>
31. Cascalho M, Platt JL. The immunological barrier to xenotransplantation. *Immunity*. 2001;14(4):437-446. [https://doi.org/10.1016/S1074-7613\(01\)00124-8](https://doi.org/10.1016/S1074-7613(01)00124-8)
32. Brown AM, Dinsley M. Graft of histocompatibility genes in sublines of inbred mice. *Nature*. 1966;212(5070):1602-1602. <https://doi.org/10.1038/2121602a0>
33. Silvers WK, Gasser DL. The genetic divergence of sublines as assessed by histocompatibility testing. *Genetics*. 1973;75(4):671-677. <https://doi.org/10.1093/genetics/75.4.671>
34. Krenkel O, Tacke F. Liver macrophages in tissue homeostasis and disease. *Nat Rev Immunol*. 2017;17(5):306-321. <https://doi.org/10.1038/nri.2017.11>
35. Schmidt-Arras D, Rose-John S. IL-6 pathway in the liver: from physiopathology to therapy. *J Hepatol*. 2016;64(6):1403-1415. <https://doi.org/10.1016/j.jhep.2016.02.004>
36. Wang J, Liu Y, Ding H, Shi X, Ren H. Mesenchymal stem cell-secreted prostaglandin E(2) ameliorates acute liver failure via attenuation of cell death and regulation of macrophage polarization. *Stem Cell Res Ther*. 2021;12(1):15. <https://doi.org/10.1186/s13287-020-02070-2>
37. Saldaña L, Bensiamar F, Vallés G, et al. Immunoregulatory potential of mesenchymal stem cells following activation by macrophage-derived soluble factors. *Stem Cell Res Ther*. 2019;10(1):58. <https://doi.org/10.1186/s13287-019-1156-6>
38. Cressman DE, Greenbaum LE, DeAngelis RA, et al. Liver failure and defective hepatocyte regeneration in interleukin-6-deficient mice. *Science*. 1996;274(5291):1379-1383. <https://doi.org/10.1126/science.274.5291.1379>
39. Peters M, Blinn G, Jostock T, et al. Combined interleukin 6 and soluble interleukin 6 receptor accelerates murine liver regeneration. *Gastroenterology*. 2000;119(6):1663-1671. <https://doi.org/10.1053/gast.2000.20236>
40. Li W, Liang X, Kellendonk C, Poli V, Taub R. STAT3 contributes to the mitogenic response of hepatocytes during liver regeneration. *J Biol Chem*. 2002;277(32):28411-28417. <https://doi.org/10.1074/jbc.M202807200>

41. Norris CA, He M, Kang LI, et al. Synthesis of IL-6 by hepatocytes is a normal response to common hepatic stimuli. *PLoS One*. 2014;9(4):e96053. <https://doi.org/10.1371/journal.pone.0096053>
42. Dewidar B, Meyer C, Dooley S, Meindl-Beinker AN. TGF- β in hepatic stellate cell activation and liver fibrogenesis—updated 2019. *Cells*. 2019;8(11):1419-1454. doi:<https://doi.org/10.3390/cells8111419>
43. Truong NH, Nguyen NH, Le TV, et al. Comparison of the treatment efficiency of bone marrow-derived mesenchymal stem cell transplantation via tail and portal veins in CCl₄-induced mouse liver fibrosis. *Stem Cells Int*. 2016;2016:5720413. <https://doi.org/10.1155/2016/5720413>
44. Khalifa YH, Mourad GM, Stephanos WM, Omar SA, Mehanna RA. Bone marrow-derived mesenchymal stem cell potential regression of dysplasia associating experimental liver fibrosis in albino rats. *Biomed Res Int*. 2019;2019:5376165. <https://doi.org/10.1155/2019/5376165>
45. Ramachandran P, Pellicoro A, Vernon MA, et al. Differential Ly-6C expression identifies the recruited macrophage phenotype, which orchestrates the regression of murine liver fibrosis. *Proc Natl Acad Sci USA*. 2012;109(46):E3186-E3195. <https://doi.org/10.1073/pnas.1119964109>
46. Choy EH, De Benedetti F, Takeuchi T, et al. Translating IL-6 biology into effective treatments. *Nat Rev Rheumatol*. 2020;16(6):335-345. <https://doi.org/10.1038/s41584-020-0419-z>
47. Rolando N, Ellis A, Degroote D, Wendon J, Williams R. Correlation of serial cytokine levels with progression to coma (grade-IV) in patients with acute liver failure (ALF). *WB Saunders Co Independence Square West Curtis Center, STE 300, Philadelphia* 1995;22(4):1038-1038.
48. Martinez JO, Evangelopoulos M, Brozovich AA, et al. Mesenchymal stromal cell-mediated treatment of local and systemic inflammation through the triggering of an anti-inflammatory response. *Adv Funct Mater*. 2021;31(3):21700192002997. <https://doi.org/10.1002/adfm.202170019>
49. Le Blanc K, Rasmusson I, Sundberg B, et al. Treatment of severe acute graft-versus-host disease with third party haploidentical mesenchymal stem cells. *Lancet*. 2004;363(9419):1439-1441. [https://doi.org/10.1016/S0140-6736\(04\)16104-7](https://doi.org/10.1016/S0140-6736(04)16104-7)
50. Zhao Y, Cooper DKC, Wang H, et al. Potential pathological role of pro-inflammatory cytokines (IL-6, TNF- α , and IL-17) in xenotransplantation. *Xenotransplantation*. 2019;26(3):e12502. <https://doi.org/10.1111/xen.12502>